Acta Crystallographica Section F
Structural Biology and Crystallization Communications
ISSN 1744-3091

Crystallization and preliminary X-ray diffraction analysis of the carbohydrate-recognizing domain (VP8*) of bovine rotavirus strain NCDV

Xing Yu,[a] Annabel Guillon,[a] Alex J. Szyczew,[a] Milton J. Kiefel,[a] Barbara S. Coulson,[b] Mark von Itzstein[a] and Helen Blanchard[a]*

[a]Institute for Glycomics, Gold Coast Campus, Griffith University, Queensland 4222, Australia, and [b]Department of Microbiology and Immunology, The University of Melbourne, Victoria 3010, Australia

Correspondence e-mail: h.blanchard@griffith.edu.au

Received 11 April 2008
Accepted 25 April 2008

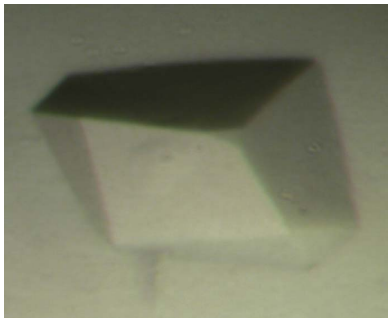

The infectivity of rotavirus is dramatically enhanced by proteolytic cleavage of its outer layer VP4 spike protein into two functional domains, VP8* and VP5*. The carbohydrate-recognizing domain VP8* is proposed to bind sialic acid-containing host cell-surface glycans and this is followed by a series of subsequent virus–cell interactions. Live attenuated human and bovine rotavirus vaccine candidates for the prevention of gastroenteritis have been derived from bovine rotavirus strain NCDV. The NCDV VP8*$_{64–224}$ was overexpressed, purified to homogeneity and crystallized in the presence of an *N*-acetylneuraminic acid derivative. X-ray diffraction data were collected to a resolution of 2.0 Å and the crystallographic structure of NCDV VP8*$_{64–224}$ was determined by molecular replacement.

1. Introduction

Rotaviruses are recognized as the leading pathogens associated with severe diarrhoea in children and young domestic animals and are responsible for more than 30% of all diarrhoea-caused hospitalizations and an estimated 600 000 infant deaths each year (Parashar *et al.*, 2006). Rotavirus-induced neonatal diarrhoea in calves occurs in many countries regardless of technology, management or sanitary procedures. Furthermore, economic loss in beef and dairy farms has driven significant efforts towards the development of vaccines and chemotherapeutic agents to control bovine neonatal diarrhoea. The Nebraska Calf Diarrhoea Virus (NCDV) strain of rotavirus has been used for cattle vaccination (Lu *et al.*, 1994). The live oral human rotavirus vaccine candidate RIT 4237 has been derived from NCDV (Vesikari *et al.*, 1984). Mature rotaviruses are non-enveloped and consist of a triple-layered particle containing a genome of 11 double-stranded RNA segments. The infectivity of some animal rotavirus strains is decreased by sialidase treatment of host cells. These 'sialidase-sensitive' strains contrast with human strains, which appear to be 'sialidase-insensitive'. It is noteworthy that sialidase treatment, for example with *Vibrio cholerae* sialidase, removes terminal sialic acids but not those that are located internally within oligosaccharide chains, such as those that can act as viral receptors on host-cell surfaces. Thus, sialidase-insensitive rotaviruses may still utilize sialic acid as part of their carbohydrate-recognition motif. Certainly, human rotavirus strains KUN and MO interact with the ganglioside GM_1 that contains an internal sialic acid during infection of MA104 monkey kidney cells (Guo *et al.*, 1999). However, whether or not this interaction involves the sialic acid moiety is unknown. Thus, the strict requirement of cell-surface sialic acid for efficient rotavirus infectivity has yet to be ascertained. Models for initial rotavirus–cell interactions suggest that sialic acid-containing receptors might be recognized as common receptors for both sialidase-sensitive and sialidase-insensitive rotavirus strains, along with integrins and heat-shock proteins (Graham *et al.*, 2003; Lopez & Arias, 2004). Both the outer layer viral spike protein (VP4) and the surface-coat protein (VP7) are involved in virus–host cell interactions at the early infection stage (Graham *et al.*, 2003; Delorme *et al.*, 2001). Rotavirus infectivity is markedly increased by trypsin treatment (Crawford *et al.*, 2001),

which cleaves VP4 into functional domains VP8* and VP5* which remain associated with the virion (Arias *et al.*, 1996). The carbohydrate-recognizing domain VP8* has essential functions in receptor binding and cell attachment and has been suggested to bind sialic acid-containing host cell-surface glycans in some strains (Fiore *et al.*, 1991; Dormitzer, Sun, Blixt *et al.*, 2002). The crystallographic structures of the VP8* domains of sialidase-sensitive rhesus rotavirus (RRV; Dormitzer, Sun, Wagner *et al.*, 2002) and porcine rotavirus strain CRW-8 (Scott *et al.*, 2005; Blanchard *et al.*, 2007) in complex with the sialic acid derivative methyl α-D-*N*-acetylneuraminide (Neu5Acα2Me) have provided some insight into the nature of sialic acid recognition by these different rotavirus strains. A site on the VP8* surface is consistent between RRV and CRW-8 in binding the sialic acid monosaccharide (Dormitzer, Sun, Wagner *et al.*, 2002; Blanchard *et al.*, 2007), but whether there is just one, or more than one, ligand-interaction site during engagement with larger oligosaccharide receptors remains to be determined. Furthermore, the ability of different strains to demonstrate specificity toward particular carbohydrates is of interest, with ganglioside-binding specificity reported as being distinct between sialidase-sensitive and sialidase-insensitive strains (Delorme *et al.*, 2001). There are also differences within sialidase-sensitive strains; for example, RRV VP8* exhibits a tenfold lower affinity for the sialic acid *N*-glycolylneuraminic acid (Neu5Gc) compared with *N*-acetylneuraminic acid (Neu5Ac); the latter has a K_d of 1.2 m*M* (Dormitzer, Sun, Blixt *et al.*, 2002). In contrast, porcine OSU (which has a VP8* with 97% sequence identity to that of CRW-8) preferably binds gangliosides containing Neu5Gc over Neu5Ac (Rolsma *et al.*, 1998). The sialidase-sensitive bovine NCDV and monkey SA11 recognize the terminal sialic acid-containing Neu5Gc-GM_3 ganglioside, but interestingly neither bound to Neu5Ac-GM_3 (Delorme *et al.*, 2001). This apparent preference for *N*-glycolyl (NHGc) over *N*-acetyl (NHAc) groups contrasts with that shown by RRV (Dormitzer, Sun, Blixt *et al.*, 2002).

As infection is triggered by rotavirus binding to host cells, it follows that suppression of this binding by competition for interaction with viral receptors will reduce virus infectivity. As the VP8* domain is involved in virus–cell interactions associated with sialic acid-containing carbohydrates, investigation into the molecular basis of the VP8*–sialic acid interaction in different rotavirus strains will further the understanding of early rotavirus-infection events and contribute to the development of rotavirus-specific therapeutics. We initiated a structural investigation to characterize the host-specificity of sialic acid recognition by the sialidase-sensitive bovine rotavirus NCDV, aiming in the first instance to explore the potential for VP8* interaction with *N*-acetyl derivatives. Here, we present the first report of the expression, purification and crystallization of bovine NCDV VP8*$_{64–224}$ together with the preliminary details of X-ray crystallographic structure determination by molecular replacement.

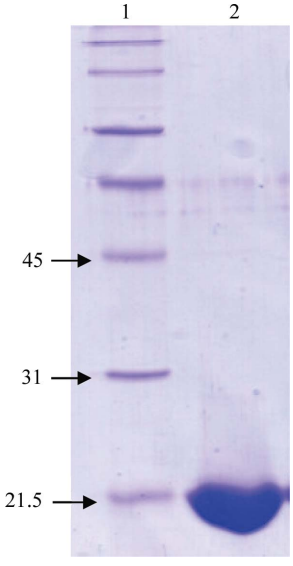

Figure 1
SDS–PAGE (12%, stained with Coomassie Blue) analysis of NCDV VP8*$_{64–224}$. Lane 1, ladder of molecular-weight standards. Lane 2, band (slightly below 21.5 kDa) representing NCDV VP8*$_{64–224}$ protein.

2. Experimental procedures and results

2.1. Expression and purification of NCDV VP8*$_{64–224}$

The NCDV VP8*$_{64–224}$ construct was provided by Dr Gavan Holloway (University of Melbourne). The amino-acid sequence of NCDV VP8*$_{64–224}$ is identical to that published (accession No. AB119636; Entrez Database, NCBI, NIH) except for the substitution of threonine by isoleucine at position 208. *Escherichia coli* strain BL21 (DE3) was transformed with pGEX-NCDV-VP8* and cells were grown at 310 K in Luria–Bertani medium supplemented with 150 µg ml^{-1} ampicillin. After reaching an OD_{600} of 0.6, the cultures were incubated at 298 K for 1 h and then induced with 1 m*M* isopropyl β-D-1-thiogalactopyranoside (BioVectra DCL). Cells were harvested after a 4 h induction by centrifugation at 6000*g* for 15 min. The supernatant was discarded and the cell pellets were frozen. Frozen cell pellets were thawed in PBS (137 m*M* NaCl, 2.7 m*M* KCl, 10 m*M* Na_2HPO_4, 2 m*M* KH_2PO_4 pH 7.3) supplemented with 0.5 m*M* phenylmethylsulfonyl fluoride (PMSF; Roche Diagnostics). The cells were lysed with 3 mg ml^{-1} lysozyme supplemented with 1%(*w*/*v*) Triton X-100 and 20 µg ml^{-1} DNaseI. After 30 min centrifugation at 20 000*g*, cell debris was removed and the supernatant was passed over a glutathione Sepharose column (Amersham-Pharmacia Biotech) and washed with TNC buffer (20 m*M* Tris pH 8.0, 100 m*M* NaCl, 1 m*M* $CaCl_2$). Proteolytic digestion was performed using 10 µg ml^{-1} TPCK-treated trypsin (Worthington Biochemical) for 2 h at room temperature. After digestion, a benzamidine Sepharose (Amersham-Pharmacia Biotech) column pre-equilibrated with TNC was connected to the glutathione Sepharose column. The N-terminal GST tag was cleaved from the protein with trypsin, leaving a remnant Gly-Ser peptide sequence, and the protein was eluted with a high-salt buffer (20 m*M* sodium phosphate pH 7.5, 1 *M* NaCl); the eluant was supplemented with 1 m*M* PMSF and 2.5 m*M* benzamidine. After dialyzing with TNE (20 m*M* Tris–HCl, 100 m*M* NaCl, 1 m*M* EDTA pH 8.0), the protein was further purified *via* size-exclusion chromatography using Sephacryl S100 resin (Sigma) pre-equilibrated with TNE. Purified VP8* protein was analysed for homogeneity by SDS–PAGE analysis (Fig. 1) and dynamic light-scattering (DLS) [DynaPro-MicroCoolBatch + 90T instrument (Precision Detectors), 293 K, protein concentration of 20 mg ml^{-1}, 20 repeats]. The DLS indicated one protein species with a hydrodynamic radius (R_h) of 1.42 nm, corresponding to monomeric NCDV VP8*$_{64–224}$, which is consistent with our previous DLS results for VP8* from rotavirus strains human Wa and CRW-8 (Kraschnefski *et al.*, 2005; Scott *et al.*, 2005). The polydispersity is 16.5% and falls in the range 15–30% that is indicative of good homogeneity.

2.2. Crystallization and X-ray diffraction data collection

NCDV VP8*$_{64–224}$ was concentrated to 20 mg ml^{-1} in TNE and mixed with an in-house-synthesized Neu5Acα2Me derivative to give a protein:ligand ratio of 1:50, which our experience with CRW-8 VP8*

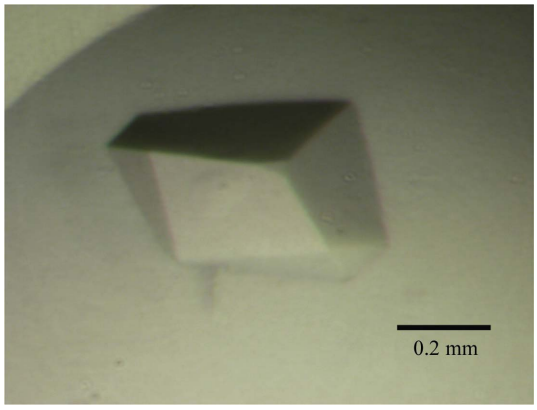

Figure 2
Crystal of NCDV VP8*$_{64–224}$ in complex with the sialic acid derivative. The resulting X-ray diffraction data (Table 1) enabled structure determination. The scale bar represents 0.2 mm.

has shown to favour complex formation (Scott *et al.*, 2005). Crystallization trials were carried out with Crystal Screen kits (Hampton Research) at 303 K using the hanging-drop vapour-diffusion method and drops comprising 1 µl protein–ligand mixture and 1 µl reservoir solution. Crystals formed in 3–5 d using reservoir solution of Crystal Screen I condition No. 35 (without further optimization), comprising 1.6 *M* sodium/potassium phosphate, 0.1 *M* HEPES pH 7.5, and grew to dimensions of 0.3 × 0.4 × 0.15 mm (Fig. 2). X-ray diffraction data were collected at room temperature (295 K) on a Bruker SMART 6000 diffractometer equipped with a SMART 6000 CCD detector and a MacScience M06X^{CE} rotating-anode generator (Cu $K\alpha$, λ = 1.5418 Å). The crystal-to-detector distance was set at 55 mm and 600 frames were collected from one crystal (no significant decay was exhibited) with an oscillation angle of 0.3° and an exposure time of 60 s. X-ray diffraction data were collected to 2.0 Å resolution (Table 1) from a capillary-mounted crystal grown in the presence of ligand (Fig. 2). Data were processed with *SAINT* (Bruker AXS, Madison, Wisconsin, USA) and scaled and merged using *SCALA* (*CCP*4 suite; Collaborative Computational Project, Number 4, 1994). The crystal exhibited a trigonal system, with unit-cell parameters $a = b = 56.28$, $c = 103.89$ Å and crystal class *P*3 or *P*32. A Matthews coefficient (Matthews, 1968) V_M of 2.64 Å^3 Da^{-1} and an associated solvent content of 53.4% were calculated for two molecules in the asymmetric unit in the lower symmetry class or for one molecule in the asymmetric unit in the higher symmetry class. A homology model of NCDV VP8*$_{64–224}$ was built using *MODELLER* (Sali & Blundell, 1993) based upon amino-acid sequence alignment and the crystal structure coordinates of porcine rotavirus CRW-8 VP8* (74% amino-acid sequence identity; PDB code 2i2s; Blanchard *et al.*, 2007). Molecular replacement was performed using *AMoRe* (Navaza, 1994). A solution was determined in space group $P3_121$, giving the anticipated single molecule in the asymmetric unit. The rotation function calculated at 15.0 to 3.0 Å resolution gave a highest rotation peak with an *R* factor of 56.4% and a correlation coefficient of 32.3%, exhibiting some distinction from the next highest peak, which had an *R* factor of 56.9% and a correlation coefficient of 30.3%. The translation-function calculation gave a highest peak correlating to the top rotation-function solution, with an *R* factor of 42.9% and a correlation coefficient of 60.3%, which are clearly distinct from those of the next highest peak, which had an *R* factor of 48.2% and a correlation coefficient of 51.9%. Rigid-body refinement was applied to this molecule and an *R* factor of 39.1% and a correlation coefficient of 71.8% were obtained. Initial refinement (ten cycles) of the structure gave an *R* factor of 28.4% and an R_{free} of 30.5%; further model building and refinement are in progress.

Table 1
X-ray diffraction data statistics.

Values in parentheses are for the highest resolution shell.

Resolution (Å)	48.74–1.99 (2.10–1.99)
Total No. of observations	81100 (4173)
Total No. of unique observations	13539 (1847)
Redundancy	5.99 (2.26)
Completeness (%)	99.2 (95.1)
Mean $I/\sigma(I)$	9.0 (2.9)
R_{merge}† (%)	6.4 (26.3)
Crystal system, space group	Trigonal, $P3_121$
Unit-cell parameters (Å, °)	$a = b = 56.28$, $c = 103.89$, $\alpha = \beta = 90$, $\gamma = 120$

† $R_{merge} = \sum_{hkl}\sum_i |I_i(hkl) - \langle I(hkl)\rangle| / \sum_{hkl}\sum_i I_i(hkl)$.

HB, MJK, BSC and MvI gratefully acknowledge the financial support of the Australian Research Council (ARC). AG thanks the Ecole de Biologie Industrielle (EBI), Paris, France for the award of an internship scholarship undertaken within the group of HB. BSC is the recipient of a Senior Research Fellowship (350253) from the National Health and Medical Research Council of Australia. MvI thanks the ARC for the award of an Australian Federation Fellowship.

References

Arias, C. F., Romero, P., Alvarez, V. & Lopez, S. (1996). *J. Virol.* **70**, 5832–5839.
Blanchard, H., Yu, X., Coulson, B. S. & von Itzstein, M. (2007). *J. Mol. Biol.* **367**, 1215–1226.
Collaborative Computational Project, Number 4 (1994). *Acta Cryst.* D**50**, 760–763.
Crawford, S. E., Mukherjee, S. K., Estes, M. K., Lawton, J. A., Shaw, A. L., Ramig, R. F. & Prasad, B. V. (2001). *J. Virol.* **75**, 6052–6061.
Delorme, C., Brussow, H., Sidoti, J., Roche, N., Karisson, K. A., Neeser, J. R. & Teneberg, S. (2001). *J. Virol.* **75**, 2276–2287.
Dormitzer, P. R., Sun, Z. Y., Blixt, O., Paulson, J. C., Wagner, G. & Harrison, S. C. (2002). *J. Virol.* **76**, 10512–10517.
Dormitzer, P. R., Sun, Z. Y., Wagner, G. & Harrison, S. C. (2002). *EMBO J.* **21**, 885–897.
Fiore, L., Greenberg, H. B. & Mackow, E. R. (1991). *Virology*, **181**, 553–563.
Graham, K. L., Halasz, P., Tan, Y., Hewish, M. J., Takada, Y., Mackow, E. R., Robinson, M. K. & Coulson, B. S. (2003). *J. Virol.* **77**, 9969–9978.
Guo, C. T., Nakagomi, O., Mochizuki, M., Ishida, H., Kiso, M., Ohta, Y., Suzuki, T., Miyamoto, D., Hidari, K. I. & Suzuki, Y. (1999). *J. Biochem. (Tokyo)*, **126**, 683–688.
Kraschnefski, M. J., Scott, S. A., Holloway, G., Coulson, B. S., von Itzstein, M. & Blanchard, H. (2005). *Acta Cryst.* F**61**, 989–993.
Lopez, S. & Arias, C. F. (2004). *Trends Microbiol.* **12**, 271–278.
Lu, W., Duhamel, G. E., Benfield, D. A. & Grotelueschen, D. M. (1994). *Vet. Microbiol.* **42**, 159–170.
Matthews, B. W. (1968). *J. Mol. Biol.* **33**, 491–497.
Navaza, J. (1994). *Acta Cryst.* A**50**, 157–163.
Parashar, U. D., Gibson, C. J., Bresse, J. S. & Glass, R. I. (2006). *Emerg. Infect. Dis.* **12**, 304–306.
Rolsma, M. D., Kuhlenschmidt, T. B., Gelberg, H. B. & Kuhlenschmidt, M. S. (1998). *J. Virol.* **72**, 9079–9091.
Sali, A. & Blundell, T. L. (1993). *J. Mol. Biol.* **234**, 779–815.
Scott, S. A., Holloway, G., Coulson, B. S., Szyczew, A. J., Kiefel, M. J., von Itzstein, M. & Blanchard, H. (2005). *Acta Cryst.* F**61**, 617–620.
Vesikari, T., Isolauri, E., D'Hondt, E., Delem, A., Andre, F. E. & Zissis, G. (1984). *Lancet*, **1**, 977–981.